

Artificial Neural Network Modelling for Wire-EDM Processing of Aluminium Silicon Carbide Metal Matrix Composite

R. A. Kapgate, V. H. Tatwawadi

Abstract— The complex phenomenon of wire electrical discharge machining (WEDM) is reducing its utilization to cut aluminium silicon carbide with 10% weight metal matrix composite (Al/SiC_{10%} MMC) for industrial applications. This paper presents an experimental investigations and development of mathematical models using ANN tool for selection of WEDM process parameters. 432 classical experiments were used to machine Al/SiC_{10%} MMC by WEDM. The selected eleven process parameters were reduced to five important dimensionless π term by using dimensional analysis. The VB based ANN tool with 5,4,1 topology and one hidden layer was developed to train, predict and optimize the data. The univariate analysis was adapted for observing the most influencing process parameters with its influencing length. The univariate ANN tool also optimized the values of range bound dimensionless π terms for maximizing material removal rate (MRR), better surface finish (Ra) and minimum electric kerf (Ek) to machine Al/SiC_{10%} MMC. The ANN tool results proved that MRR, Ra and Ek values were significantly influenced by changing important π_2 , π_4 and π_5 dimensionless π terms. These dimensionless π terms were suggested the effective guidelines to the manufacturer for improving productivity by changing any one or all from the available process parameters.

Index Terms— Stir casting, Al/SiC_{10%} MMC, Dimensional analysis, Buckingham's π theorem, Feed forward back propagation ANN tool, 1h ANN topology, Sigmoidal function, Univariate analysis.

1 INTRODUCTION

Presently aluminium based composites with SiC and Al₂O₃ particles are attracted for many engineering industrial applications because of their high temperature strength, fatigue strength, damping strength, wear resistance and low friction coefficient [1]. However, machining of Al/SiC_{10%} MMCs using conventional tool materials is very difficult due to presence of abrasive reinforcing phase which causes severe tool wear [2],[3],[4]. Recently wire electrical discharge machining (WEDM) widely used in industries for precise, complex and irregular shapes of difficult-to-machine electrically conductive materials. In this operation, the material removal occurs by the ignition of rapid and repetitive spark discharges between the gaps of workpiece and tool electrode connected in an electric circuit. A small wire of diameter 0.05 -0.3 mm is continuously supplied from spool to work piece with a maintained gap of 0.025-0.05 mm between wire and workpiece [5],[6],[7]. Because of complicated stochastic process mechanism of machining, the selection of process parameters for obtaining higher cutting efficiency and accuracy is still not fully solved, even with the most up-to-date CNC WEDM machine [8]. Scot et al. [9] found that discharge current, pulse duration and pulse frequency were main significant control parameters for better MRR and surface finish. Trang et al. [10] utilized a neural network to model the WEDM process to assess the optimal cutting parameters.

Literature lacks much to say about the use of WEDM for machining Al/SiC_{10%} MMC, so the need has been felt towards the highlighting the process with the goal of achieving mathematical models to select the process parameters for maximum utilization of WEDM with improved process performance.

The present work highlights the development of mathematical models for correlating the inter relationships of various WEDM process parameters to optimize MRR, Ra and Ek of Al/SiC_{10%}

MMC. This work has been established on the artificial neural network (ANN) approach. Mathematical models developed by ANN fitted to the experimental data were contribute towards the selection of the maximum, minimum and optimum process conditions.

2 EXPERIMENTAL PROCEDURES

Discontinuous reinforced Al/SiC_{10%} MMC made up by stir casting route [11],[12] with SiC average particle size 45 μ m was used for experimentation. Different sets of 432 machining experiments were performed on SODICK 350W CNC WEDM with MARK 21 controller (Fig.1). The electrode and other machining conditions were selected as follows-

- i. Electrode: Brass with 0.25mm in dia.
- ii. Specific resistance of die-electric fluid, Ω cm : 5×10^4
- iii. Workpiece height: 5 and 10mm
- iv. Die electric temperature, $^{\circ}$ C : 25-30

Pilot experiments were performed to select test envelope and test points of process parameters for experimental design. These process parameters were listed in Table 1 and used in experimental design for the investigation of WEDM process parameters during machining of Al/SiC_{10%} MMC. All eleven selected independent process parameters were manipulated on WEDM control panel and accordingly 2mm, 4mm and 6mm length triangular, circular and rectangular shape (Fig.2) were machined. During machining cutting speed (V_c), gap current (I) and gap voltage (V) were measured from control panel. Surface finish (Ra, μ m) was measured by using Surf Test- 300 (Mitituyo make) and the width of cut (b) was measured by using tool makers' microscope. The MRR was calculated [13] as:

$$MRR = V_c * b * h \text{ m}^3/\text{s} \text{-----} (1)$$

Where, V_c =cutting speed, m/s,

b=width of cut, m

h= height of work piece, m

R.A. Kapgate, Research scholar, Department of Mechanical Engg, Priyadarshini College of Engineering, Nagpur, India,
Dr.V.H. Tatwawadi, Principal, Dr. Babasaheb Ambedkar college of engineering and Research, Wanadongari, Nagpur, India,



Fig. 1: Experimental Set Up

Table 1: Process Parameters

Sr. No	Machining parameters	Abbreviation	Selected values	Unit
i.	Pulse on time	ON	0.5,2,4,6	µs
ii	Pulse off time	OFF	12,14,16,18	µs
iii.	Main power supply peak current	IP	16,17	A
iv	Servo reference voltage	SV	90,100,110,120	V
v	Servo speed	SS	6.66*10 ⁻⁵ , 3.33*10 ⁻⁵ , 0.000125, 0.00025	m/s
vi	Wire tension	WT	12,18	N
vii	Wire speed	WS	0.083333, 0.116667, 0.15	m/s
viii	Dielectric fluid flow	DQ	8.33333*10 ⁻⁵ , 0.0001166	m ³ /s
ix	Al/SiC work-piece thickness	MT	0.005, 0.01	M
x	Al/SiC work-piece length	ML	0.002, 0.004, 0.006	M
xi	Al/SiC work-piece cross section	MS	Angular, circular, straight	M

3 DESIGN OF EXPERIMENTS

In this study, 432 experiments were designed on the basis of sequential classical experimental design technique [14] that has been generally proposed for engineering applications. The basic classical plan [15] consists of holding all but one of the independent variables constant and changing this one variable over its range

The main objective of the experiments consists of studying the relationship between 11 independent process parameters with the MRR, Ra and Ek dependent responses. Simultaneous changing of all 11 independent parameters was cumbersome and confusing in industrial applications. Hence all 11 independent process parameters were reduced by dimensional analysis. Buckingham's π theorem

was adapted to develop dimensionless π terms for reduction of process parameters.

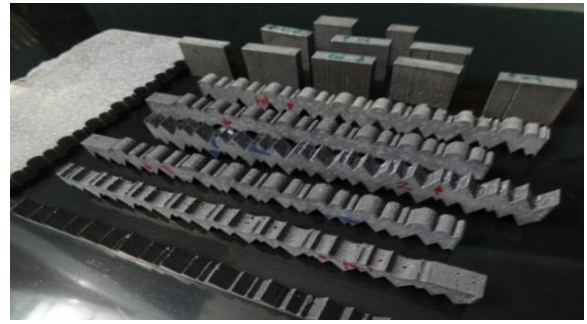


Fig. 2: Machining of Al/SiC MMC using WEDM

Artificial neural network modeling used to better understand how the change in the levels of any one process parameter of a π terms changed MRR, Ra and Ek responses. A combination of the levels of dimensionless π terms, which lead to maximum, minimum and optimum response, can also be located through this approach. ANN models of MRR, Ra and Ek were optimized by mini-max principle.

3.1 FORMULATION OF PI TERMS BY DIMENSIONAL ANALYSIS

As per dimensional analysis [15], material removal rate (MRR) was written in the function form as
 $f_1 = (ON, OFF, IP, SV, SS, WT, WS, DQ, MT, ML, MS, MRR) = 0$ ----- (2)

By selecting Mass (M), Length (L), Time (θ) and Current (I) as the basic dimensions, the basic dimensions of the forgoing quantities were:

ON= θ, OFF= θ, IP= I, SV= L²M θ⁻³I⁻¹, SS= L θ⁻¹, WT= ML θ⁻², WS = L θ⁻¹, DQ= L³ θ⁻¹, MT= L, ML = L, MS= L, MRR= L³ θ⁻¹, SF=L

According to the Buckingham's π- theorem, (n- m) number of dimensionless groups [16] are forms. In this case n is 12 and m=4, so we were form π₁ to π₈ dimensionless groups. By choosing ON, IP, WT, and DQ as a repeating variable, eight π terms were developed as follows:

π₁= (ON)^{a₁} * (IP)^{b₁} * (WT)^{c₁} * (DQ)^{d₁} * OFF
 π₂= (ON)^{a₂} * (IP)^{b₂} * (WT)^{c₂} * (DQ)^{d₂} * SV
 π₃= (ON)^{a₃} * (IP)^{b₃} * (WT)^{c₃} * (DQ)^{d₃} * SS
 π₄= (ON)^{a₄} * (IP)^{b₄} * (WT)^{c₄} * (DQ)^{d₄} * WS
 π₅= (ON)^{a₅} * (IP)^{b₅} * (WT)^{c₅} * (DQ)^{d₅} * MT
 π₆= (ON)^{a₆} * (IP)^{b₆} * (WT)^{c₆} * (DQ)^{d₆} * ML
 π₇= (ON)^{a₇} * (IP)^{b₇} * (WT)^{c₇} * (DQ)^{d₇} * MS
 π₈= (ON)^{a₈} * (IP)^{b₈} * (WT)^{c₈} * (DQ)^{d₈} * MRR

By substituting the dimensions of each quantity and equating above π terms to zero and using dimensional analysis method equation 2 becomes,

0 = f₁(π₁, π₂, π₃, π₄, π₅, π₆, π₇, π₈) ----- (3)

Since 5th, 6th & 7th π term had same denominator.

Hence,
 0 = f₁(π₁, π₂, π₃, π₄, π₅, π₈) ----- (4)

π₈ = f₁(π₁, π₂, π₃, π₄, π₅) ----- (5)

Where,

π₁=(OFF/ON);
 π₂= ((ON^{2/3} * IP * SV) / (DQ^{1/3} * WT));

$$\begin{aligned} \pi_2 &= ((ON^{2/3} * SS) / (DQ^{1/3})); \\ \pi_4 &= ((ON^{2/3} * WS) / (DQ^{1/3})); \\ \pi_5 &= ((MT * ML * MS) / (ON^{2/3} * DQ^{1/3})); \\ \pi_8 &= ((MRR) / (DQ)) \end{aligned}$$

Hence dimensional analysis reduced 12 independent and dependent variables into only six dimensionless π terms.

Similarly, dimensionless π terms for surface finish (Ra) and electric kerf (Ek) were found by dimensional analysis,

$$\pi_9 = f_1(\pi_1, \pi_2, \pi_3, \pi_4, \pi_5) \text{----- (6)}$$

And

$$\pi_9 = ((Ra) / (ON^{2/3} * DQ^{1/3}))$$

Similarly,

$$\pi_{10} = f_1(\pi_1, \pi_2, \pi_3, \pi_4, \pi_5) \text{----- (7)}$$

And

$$\pi_{10} = ((Ek) / (ON^{1/3} * DQ^{1/3}))$$

The relationship between various parameters was unknown. The dependent parameter i.e. π_8, π_9 and π_{10} relating to MRR, Ra and Ek were bear an intricate relationship with remaining $(\pi_1, \pi_2, \pi_3, \pi_4, \pi_5)$ terms evaluated on the basis of experimentation. The true relationship was difficult to obtain.

This relationship now can be viewed as the hyper plane in five dimensional spaces. To simplify further let us apply ANN methodology for analysis.

3.2 ANN MODEL DEVELOPMENT

The ANN is capable of performing nonlinear mapping between the input and output space parameters due to its large parallel interconnection between different layers and the nonlinear processing characteristics. An artificial neuron basically consists of a computing element that performs the weighted sum of the input signal and the connecting weight. The sum is added with the bias or threshold. And the resultant signal is then passed through a nonlinear function of sigmoid or hyperbolic tangent type. Each neuron is associated with three parameters whose learning can be adjusted; these are the connecting weights, the bias and the slope of the nonlinear function. For the structural point of view a neural network may be single layer or it may be multilayer. In multilayer structure, there is one or many artificial neurons in each layer and for a practical case there may be a number of layers. Each neuron of the one layer is connected to each and every neuron of the next layer. The basic ANN model is as shown in figure 3.

3.2.1 Feed forward back propagation Neural Network model

The mathematical models for MRR, Ra and Ek were dedeveloped by feed forward back propagation ANN model. The neural network used in this case was predictive in nature with supervised learning. It was range bound for all input factors. In neural network terminology total input and output cells were 10. As per the dimensional analysis total input parameters were five and network with one hidden layers was reasonable to simulate i.e.1 h ANN topology (Fig.3). All five dimensionless π terms were scaled down between zero and one using their maximum and minimum values as given.

Scaled values =

$$(Current\ value - Min.\ value) / (max.\ value - min.\ value)$$

This is the requirement to make the data flow on neural network. Initially the values of synaptic weights and thresholds were chosen randomly between zero and one. The prevailing value (pv) of each perceptron was calculated by hyperbolic tan function.

$$pv(31) = (1 - e^{-s}) / (1 + e^{-s})$$

The pv values iterated forward and backward to achieve accuracy at sixth place of decimal. The weights and threshold were corrected in every iteration. The values of weights and thresholds obtained at the end were matured values and indicated the end of learning process of the network.(Table 3 , 4).

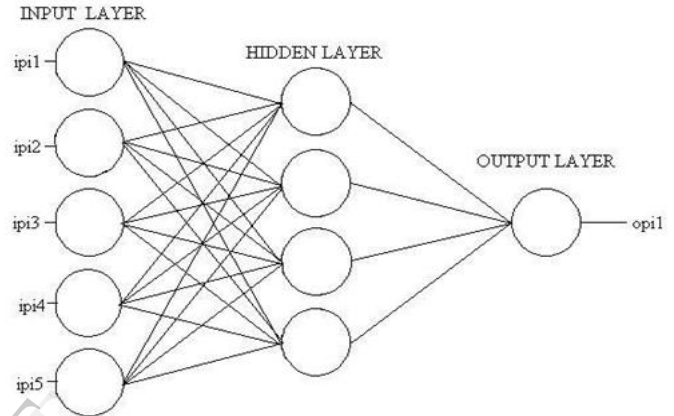


Figure 3: Basic ANN Model

Thus it was very easy to answer what would be the output parameter if input factors were known. A separate VB base program was written for this prediction. This program simulated the structure (Fig. 3) of entire network using final values of weights and thresholds. It carried out the single iteration using scaled values of input factors to generate the scaled values of output parameter. This scaled value was further translated to its physical value by reverse scaling calculations. In this way once the network went through the learning process, it was capable of predicting output parameters viz. matrial removal rate , surface finish and electric kerf immediately. The complex relationship in manipulation of the output was not truly known but the numerical results were obtainable. Moreover these results were least affected by discrepant error.

3.2.1.1 Training to ANN model for MRR

The output MRR (opi1) was developed by computing the weights and threshold values from node of first layer to the connected other nodes of hidden and output layers. The details of training the ANN model as given in table 2.

Table 2: ANN parameters used to train the ANN network

Sr. No.	Parameters	ANN training values
1	Number of hidden layer	01
2	Learning factor	0.01
3	Transfer function used	Sigmoidal
4	Number of hidden neurons	4
5	Number of epochs	10000
6	Momentum factor	0.5

Table3: Weights and thresholds of all nodes from layer 1 to layer 2

	1	2	3	4	5	Threshold				
1	-101.05	9.732891	18.9216	2.686327	-0.9887	93.88503	*	=	$\begin{matrix} S_{1,1} \\ S_{1,2} \\ S_{1,3} \\ S_{1,4} \end{matrix} \text{ transform by } \begin{matrix} X_{1,1} \\ X_{1,2} \\ X_{1,3} \\ X_{1,4} \end{matrix}$ $(1 - e^{-1 * S_{1,i}}) / (1 - e^{-1 * S_{1,i}})$	
2	-24.72	-2.36443	0.656152	-4.06412	21.70783	$X_{0,1}$				$X_{1,1}$
3	-14.5999	-2.89046	8.997999	4.803129	2.56823	$X_{0,2}$				$X_{1,2}$
4	35.76814	3.16876	-5.9203	4.28675	2.174713	$X_{0,3}$				$X_{1,3}$
						$X_{0,4}$				$X_{1,4}$
						$X_{0,5}$				
						-1				

Table4: Weights and thresholds of all nodes from layer 2to layer 3

	1	2	3	4	Threshold					
1	0.435345	0.492075	1.208969	-0.64691	0	*	=	$S_{2,1} \text{ transform by } \begin{matrix} X_{2,1} \end{matrix}$ $(1 - e^{-1 * S_{2,i}}) / (1 - e^{-1 * S_{2,i}})$		
									$X_{1,1}$	$X_{2,1}$
									$X_{1,2}$	
									$X_{1,3}$	
									$X_{1,4}$	
						-1				

Figure 4: ANN Topology of MRR

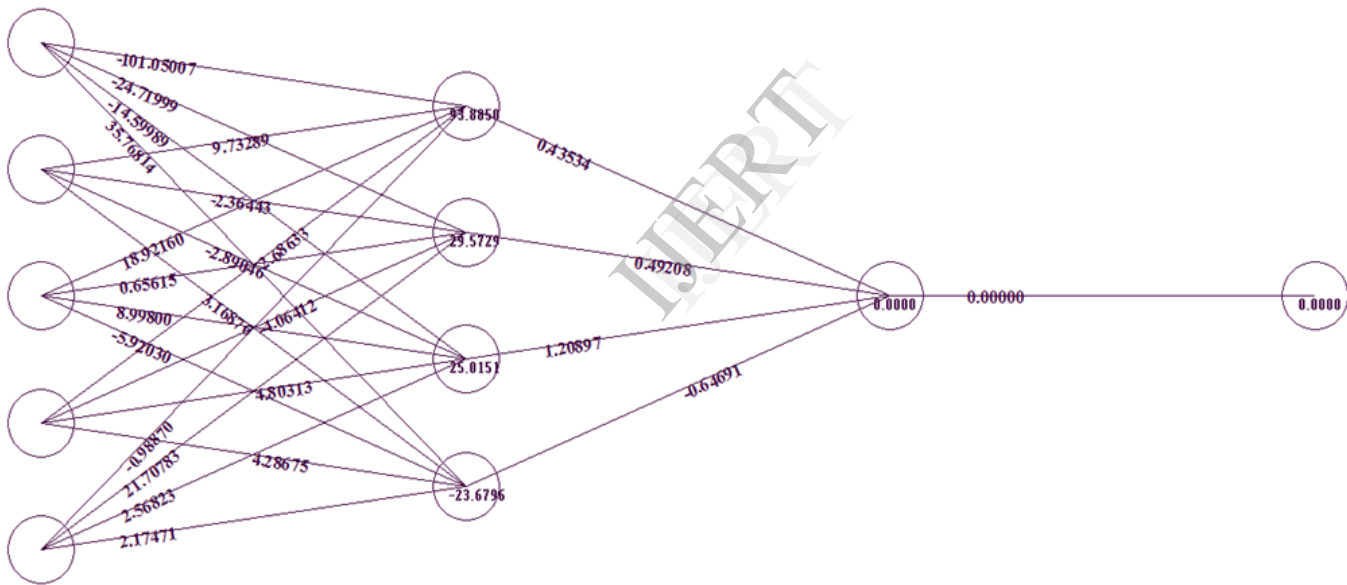
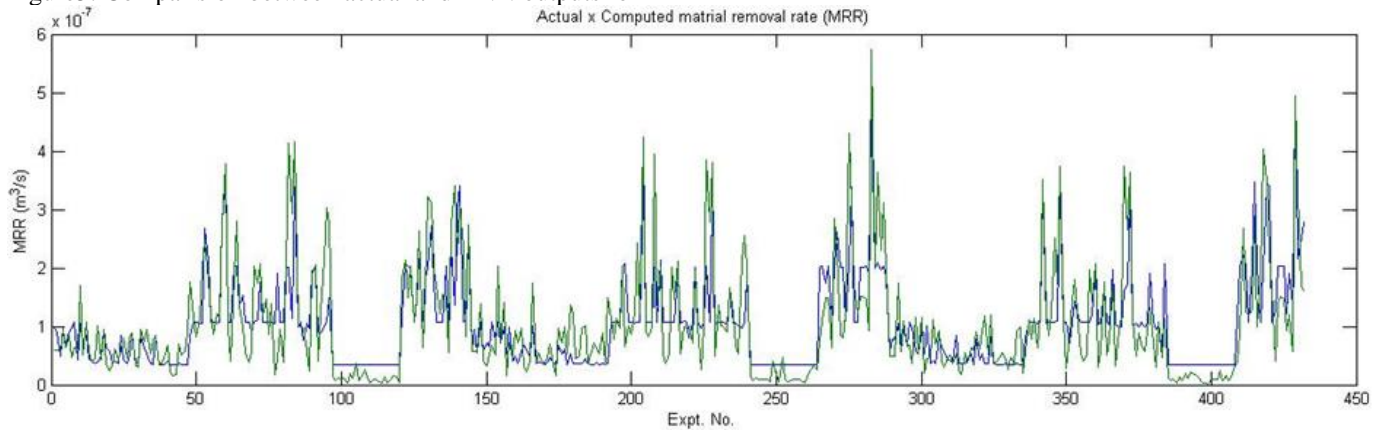


Figure5: Comparison between actual and ANN outputs for MRR



The weights and threshold values were given in Table 3 and 4. Hence after training to the ANN model an ANN equation was developed as

$$opi1 = (1 - e^{-1 * \text{sum}(\text{layer 2 cell } 0)}) / (1 - e^{-1 * \text{sum}(\text{layer 2 cell } 0)})$$

Where, $\text{sum}(\text{layer 2 cell } 0) = 0.435344673 * X_{1,1} + 0.49207543 * X_{1,2} + 1.208969181 * X_{1,3} - 0.646909037 * X_{1,4} - 0.0000000$

And $X_{1,1}, X_{1,2}, X_{1,3}, X_{1,4}$ were computed from Table 2 as follows :

$$X_{1,1} = (1 - e^{-1 * \text{sum}(\text{layer 1 cell } 0)}) / (1 - e^{-1 * \text{sum}(\text{layer 1 cell } 0)})$$

Where, $\text{sum}(\text{layer 1 cell } 0) = -101.0500693 * X_{0,1} + 9.732891283 * X_{0,2} + 18.92160414 * X_{0,3} + 2.68632748 * X_{0,4} - 0.988699129 * X_{0,5} - 93.88502863$

$$X_{1,2} = (1 - e^{-1 * \text{sum}(\text{layer 1 cell } 1)}) / (1 - e^{-1 * \text{sum}(\text{layer 1 cell } 1)})$$

Where, $\text{sum}(\text{layer 1 cell } 1) = -24.71998941 * X_{0,1} - 2.364433503 * X_{0,2} + 0.656152358 * X_{0,3} - 4.064121616 * X_{0,4} + 21.70782525 * X_{0,5} - 29.57289105$

$$X_{1,3} = (1 - e^{-1 * \text{sum}(\text{layer 1 cell } 2)}) / (1 - e^{-1 * \text{sum}(\text{layer 1 cell } 2)})$$

Where, $\text{sum}(\text{layer 1 cell } 2) = -14.59988996 * X_{0,1} - 2.890455464 * X_{0,2} + 8.997999049 * X_{0,3} + 4.803129141 * X_{0,4} + 2.568229507 * X_{0,5} - 25.01508634$

$$X_{1,4} = (1 - e^{-1 * \text{sum}(\text{layer 1 cell } 3)}) / (1 - e^{-1 * \text{sum}(\text{layer 1 cell } 3)})$$

Where, $\text{sum}(\text{layer 1 cell } 3) = 35.76814034 * X_{0,1} + 3.168759738 * X_{0,2} - 5.920299799 * X_{0,3} + 4.286749827 * X_{0,4} + 2.17471322 * X_{0,5} + 23.67960855$

The corelaion and root mean square error of the model was 0.815868 and 0.0000000624 respectively.

By using similar approach ANN models for Ra naluves were developed.

3.2.1.2 Training to ANN model for Ra

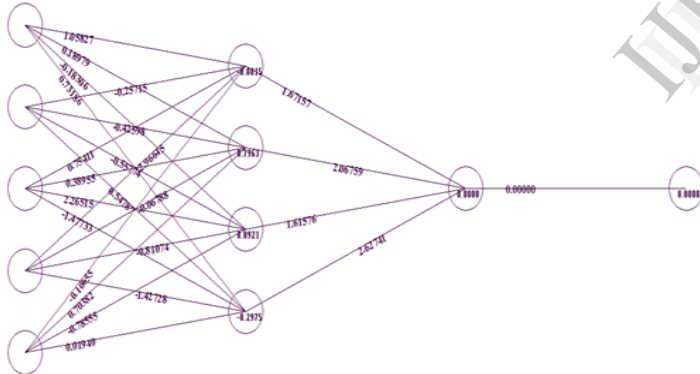


Figure 6 : ANN topology for Ra

The output Ra (opi2) was developed by computing the weights and threshold values from node of first layer to the connected other nodes of hidden and output layers(Fig.6). The training to the ANN model was given the equation for opi2 as follows

$$opi2 = (1 - e^{-1 * \text{sum}(\text{layer 2 cell } 0)}) / (1 - e^{-1 * \text{sum}(\text{layer 2 cell } 0)})$$

Where, $\text{sum}(\text{layer 2 cell } 0) = 1.67157 * X_{1,1} + 2.067592 * X_{1,2} + 1.615761 * X_{1,3} + 2.627413 * X_{1,4} + 0.00000$

And $X_{1,1}, X_{1,2}, X_{1,3}, X_{1,4}$ were computed as follows :

$$X_{1,1} = (1 - e^{-1 * \text{sum}(\text{layer 1 cell } 0)}) / (1 - e^{-1 * \text{sum}(\text{layer 1 cell } 0)})$$

Where, $\text{sum}(\text{layer 1 cell } 0) = 1.058274 * X_{0,1} - 0.25715 * X_{0,2} + 0.75411 * X_{0,3} + 2.966452 * X_{0,4} - 0.10655 * X_{0,5} + 0.80149$

$$X_{1,2} = (1 - e^{-1 * \text{sum}(\text{layer 1 cell } 1)}) / (1 - e^{-1 * \text{sum}(\text{layer 1 cell } 1)})$$

Where, $\text{sum}(\text{layer 1 cell } 1) = 0.189792 * X_{0,1} - 0.42598 * X_{0,2} + 0.389551 * X_{0,3} - 0.06788 * X_{0,4}$

$$X_{1,3} = (1 - e^{-1 * \text{sum}(\text{layer 1 cell } 2)}) / (1 - e^{-1 * \text{sum}(\text{layer 1 cell } 2)})$$

Where, $\text{sum}(\text{layer 1 cell } 2) = -0.18306 * X_{0,1} - 0.55774 * X_{0,2} + 2.265147 * X_{0,3} - 0.81074 * X_{0,4} - 0.78555 * X_{0,5} - 0.092133$

$$X_{1,4} = (1 - e^{-1 * \text{sum}(\text{layer 1 cell } 3)}) / (1 - e^{-1 * \text{sum}(\text{layer 1 cell } 3)})$$

Where, $\text{sum}(\text{layer 1 cell } 3) = 0.731863 * X_{0,1} + 0.547867 * X_{0,2} - 1.47733 * X_{0,3} - 1.42728 * X_{0,4} + 0.019396 * X_{0,5} + 0.29746$

The comparision between experimental and computed error of the ANN model for Ra is given in figure7. While the corelaion and root mean square error of the model was 0.844417 and 0.0011 respectively.

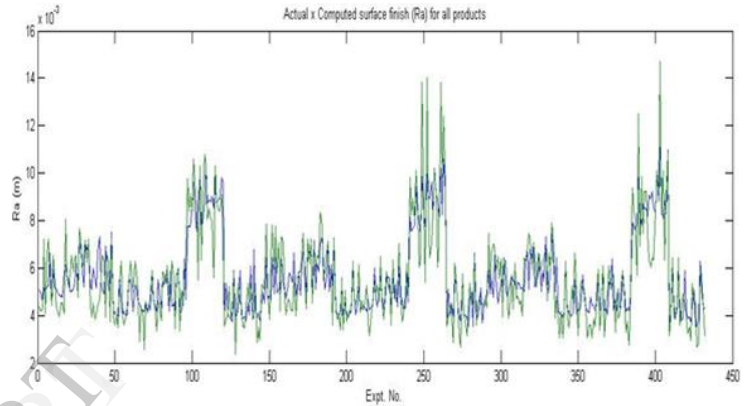


Figure 7: Comparison between experimental and Computed ANN values for Ra

3.2.1.3 Training to ANN model for Ek

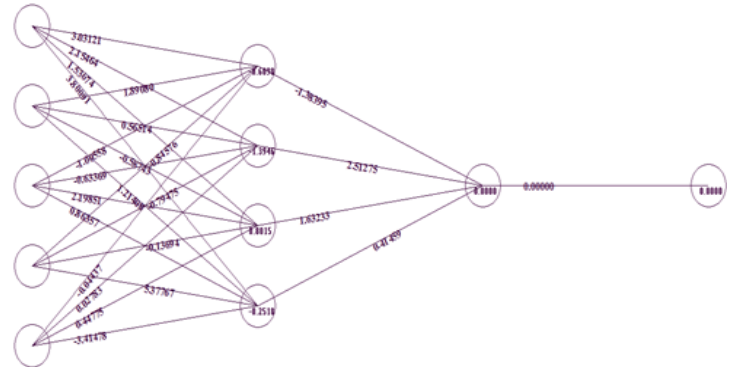


Figure 8 : ANN topology for Ek

The output Ek (opi3) was developed by computing the weights and threshold values from node of first layer to the connected other nodes of hidden and output layers(Fig.8). The training to the ANN model was given the equation for opi3 as follows

$$Opi3 = (1 - e^{-1 * \text{sum}(\text{layer 2 cell } 0)}) / (1 - e^{-1 * \text{sum}(\text{layer 2 cell } 0)})$$

Where, $\text{sum}(\text{layer 2 cell } 0) = -1.38395 * X_{1,1} + 2.512747 * X_{1,2} + 1.632333 * X_{1,3} + 0.414591 * X_{1,4} + 0.00000$

And $X_{1,1}, X_{1,2}, X_{1,3}, X_{1,4}$ were computed as follows :

$$X_{1,1} = (1 - e^{-1 * \text{sum}(\text{layer 1 cell } 0)}) / (1 - e^{-1 * \text{sum}(\text{layer 1 cell } 0)})$$

Where, $\text{sum}(\text{layer 1 cell } 0) = 3.03121 * X_{0,1} + 1.8908 * X_{0,2} - 1.00558 * X_{0,3} - 0.84576 * X_{0,4} - 0.04437 * X_{0,5} - 0.60978$

$$X_{1,2} = (1 - e^{-1 * \text{sum}(\text{layer 1 cell } 1)}) / (1 - e^{-1 * \text{sum}(\text{layer 1 cell } 1)})$$

Where, $\text{sum}(\text{layer 1 cell } 1) =$

$$X_{1,3} = \frac{2.154639 * X_{0,1} + 0.565142 * X_{0,2} - 0.63369 * X_{0,3} - 0.79475 * X_{0,4} + 0.027828 * X_{0,5} - 1.39463}{(1 - e^{-1 * \text{sum}(\text{layer 1 cell 2})}) / (1 - e^{-1 * \text{sum}(\text{layer 1 cell 2})})}$$

Where, sum (layer1 cell 2) =

$$X_{1,4} = \frac{1.536739 * X_{0,1} - 0.58743 * X_{0,2} + 2.198514 * X_{0,3} - 0.13694 * X_{0,4} + 0.44775 * X_{0,5} + 0.801512}{(1 - e^{-1 * \text{sum}(\text{layer 1 cell 3})}) / (1 - e^{-1 * \text{sum}(\text{layer 1 cell 3})})}$$

Where, sum (layer1 cell 3) =

$$3.800913 * X_{0,1} + 1.21408 * X_{0,2} + 0.863574 * X_{0,3} + 5.377673 * X_{0,4} - 3.41478 * X_{0,5} - 0.25185$$

The comparison between experimental and computed error of the ANN model for Ek is given in figure9. While the correlation and root mean square error of the model was 0.844417 and 0.0011 respectively.

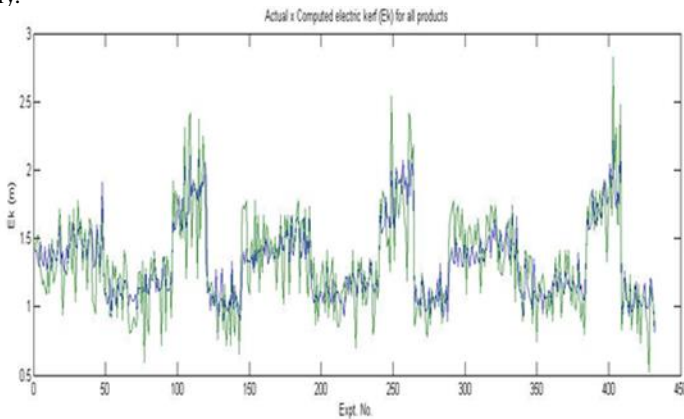


Figure 9: Comparison between experimental and Computed ANN values for Ek

3.3 PREDICTION OF OUTPUTS BY ANN PREDICTION TOOL

The relationship was developed through ANN modeling was not sufficient because it was mere a training to the model. Hence prediction was necessary to predict the output from the trained data.

The predictive tool was developed on supervised learning process with feed forward back propagation ANN model. After the training of the ANN model, prediction of any experiment was carried out to find the output at the same experiment. The predictive tool was given the output (opi2) for experiment number 376 as 0.00060654 with error 0.00031. (Fig.10)

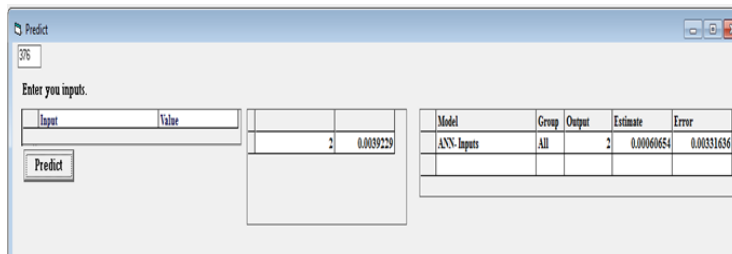


Figure 10: prediction tool of ANN model

3.4 OPTIMAL SOLUTION FOR ANN MODELS

Optimization in case of ANN models was carried out using univariate analysis approach. This was the method for deciding highly influential input parameters. It primarily computed differential dy/dx values for all inputs. Here the

value of one of the x variable was increased by 0.01 and change in output was recorded. After computing in this manner for all variables the order sequence of influence was obtained. It was provided the better insight to interaction process and variables. In order to decrease the output most dominating factor was incremented. Sensitivity was checked after every increment. This process ended when output did not decrease or the range to which any input variable can be incremented was exhausted.

In ANN model the input values were scaled between -1 to 1. By using univariate analysis most influencing variable and its length of influence was determined. Initially randomly selected first parameter was shown maximum influence but after certain length of maximum influence of input variable some other input variable may turn out to be maximum influential. This way when either all input variables were reached to maximum value i.e.1 or value of output did not improved then optimal solution was obtained.

For the MRR most influential input parameter was ipi3 and optimal solution was computed as table 5.

Table 5 : optimized value of MRR

Sr No.	Input variable	Opt. values	Max. Values
1	ipi1	6	6
2	ipi2	0.290739295	0.290739295
3	ipi3	1.30376E-07	1.21141E-07
4	ipi4	0.000302853	0.000302853
5	ipi5	0.00002	0.00002
Optimum soln		9.94886E-08	5.7528E-07

For the Ra most influential input parameter were ipi2, ipi 4 and ipi5 with influential length 168, 45, and 44 consecutively. The optimal solution was computed as table 6.

Table6: Optimized value of Ra

Sr. No.	Input variable	Opt. values	Min. Values
1	ipi1	6	6
2	ipi2	1.283603261	0.290739295
3	ipi3	1.21141E-07	1.21141E-07
4	ipi4	0.000533814	0.000302853
5	ipi5	0.000042946	0.00002
Optimum soln		0.004044575	0.014710946

For the Ek most influential input parameter were ipi4 and ipi5 with influential length 61 and 59 (Table7) consecutively. The optimal solution was computed as table 8.

3.5 RESULTS AND DISCUSSION

3.5.1 Development of π terms

The Buckingham's 'π' theorem formulated six dimensionless π terms and each π term was given the importance of each dimensionless group. The first π term implied the effect of spark frequency of wire EDM process on MRR, Ra and Ek values. The second π term showed the importance of spark energy supplied

to the wire so as to minimize the breakage of wire which has taken a major non-productive time during WEDM. Third, fourth and fifth π terms were relate with the role of servo speed, wire speed and product variability during machining. Finally the last π term reflected the outputs MRR, Ra and Ek responses.

Table 7: Most influential input parameter for Ek

Output var	Revolution	Influence length	pi_var	op. value
opi4	1	52	4	1.305338
opi4	2	59	5	1.260094
opi4	3	40	4	1.190099
opi4	4	61	5	1.142835
opi4	5	40	4	1.075545
opi4	6	61	5	1.031752
opi4	7	29	4	0.98016
opi4	8	10	5	0.971729

Table 8: Optimal solution for Ek

Sr. No.	Input variable	Opt. values	Min. Values
1	ipi1	6	6
2	ipi2	0.290739295	0.290739295
3	ipi3	1.21141E-07	1.21141E-07
4	ipi4	0.00112918	0.000302853
5	ipi5	0.000119607	0.00002
Optimum soln.		0.971729385	2.826809158

3.5.2 ANN modelling for MRR

Mathematical model was developed by using sigmoidal function in the the ANN Programme. This ANN program provided 5,4,1 ANN topology for the MRR and also suggested the values of weights and threshold in the topology for calculating the prevailing values of each node and for calculating the computed response of the MRR. The wights and threshold values were given the table 3 from input layer to hidden and in table 4 was showed the above values from hidden layer to final computed layer. From the table 3 , threshold values for node 1 of hidden layer was 93.88503 while the weights accumulated to the above said node were -101.05 ,9.732891, 18.9216, 2.686327and -0.9887 hence the pv values were very easily calculated. The prediction tool was greatly used for predicting any values of the experiments and also provided the error within experimental and predicted values of the ANN model. Finally univariate analysis of the ANN model suggested the sensitivity of the mathematical model with 0.01 differetial and gave most influential process parameter for better effect on MRR. The univariate process suggested that ipi3 (servo speed) parameter was more influencing on MRR. This ipi3 meant the $\pi_3 = ((ON^{2/3} * SS) / (DQ^{1/3}))$ and it was directly influencing the maximum values of MRR. Since this was the ratio hence by increasing spark on (ON) value or servo speed (SS) MRR was increased. The optimization of ANN model was also suggested by the univariate process. The input process parameters with optimized MRR of 9.94886E-08 m³/s were given in table 5 which was better than computed maximum MRR for

the same mathematical model of ANN.

3.5.3 ANN modelling for Ra

The 432 experimental data was trained in 5, 4, 1 topology of ANN programme. In this prograame one hidden layer was used and developed topology was calculating the weights and thresolds of every perceptron. The prevailing values (pv) of each perceptron were used to caluculate the computed Ra values. The mathematical model suggested by this ANN programme was $opi2 = (1 - e^{-1 * \text{sum}(\text{layer 2 cell 0})}) / (1 - e^{-1 * \text{sum}(\text{layer 2 cell 0})})$ Where, $\text{sum}(\text{layer 2 cell 0}) = 1.67157 * X_{1,1} + 2.067592 * X_{1,2} + 1.615761 * X_{1,3} + 2.627413 * X_{1,4} + 0.00000$. This equation calculated the computed Ra values and also helpful for prediction programme of the ANN. The predicted values of any experiment were calculated very easily just by inserting the experiment number into prediction ANN programme. The univariate programme of the ANN was concluded about the sensitivity of the model and optimized values of the computed Ra. The Ra was greatly influential by input parameter ipi2, ipi 4 and ipi5 with influential length 168, 45, and 44 consequetively . The ipi2 means spark energy supplied during WEDM process and the parameters included into this terms were $\pi_2 = ((ON^{2/3} * IP * SV) / (DQ^{1/3} * WT))$. This was sugessted that just by increasing ON or IP or SV values machining process can improve the Ra values. Similarly ipi4 and ipi5 means wire speed factor and product variability. It was concluded that if the wire speed increased then Ra improves. And product variability sugessted that if shape changed then also Ra changed. The optimized values of Ra were calculated by ANN optimize programme as 0.004044575 μm .

3.5.4 ANN modelling for Ek

The ANN training to the experimental data was given the mathemaical equation for $opi3 = (1 - e^{-1 * \text{sum}(\text{layer 2 cell 0})}) / (1 - e^{-1 * \text{sum}(\text{layer 2 cell 0})})$ Where , $\text{sum}(\text{layer 2 cell 0}) = -1.38395 * X_{1,1} + 2.512747 * X_{1,2} + 1.632333 * X_{1,3} + 0.414591 * X_{1,4} + 0.00000$. This training also used 5,4,1 ANN topology with one hidden layer. The output data of ANN training tool was used for prediction of Ek values. Finally the univariate analysis suggested that ipi4 and ipi5 were most influencing factors with influential length adjustment from 52 to 29 and 61 to 10. The optimized value of Ek was 0.971729385 m which was better than minimized values of equation.

3.6 CONCLUSION

The true power and advantage of neural networks lies in their ability to represent both linear and non-linear relationships and in their ability to learn these relationships directly from the data being modelled. Hence use of ANN tool concluded that-

1. WEDM process has proved its adequacy to machine Al/SiC_{10%} MMC under acceptable volumetric material removal rate (MRR) which was reached upto 9.94886E-08 m³/s, surface finish (Ra) 0.004044575 μm and electric kerf (Ek) 0.971729385 m.
2. The dimensionless π terms have provided the idea about combined effect of process parameters in that π terms. A simple change in one process parameter in the group helped the manufacturer to maintain the required MRR and Ra values so that the productivity improved.

3. The mathematical models developed after training to 5,4,1 ANN topology with one hidden layer were useful for predicting the characteristics of Wire electric discharge machining and this models could be effectively utilized for prediction of machining parameters of Al/ SiC_{10%} MMCs in wide spread engineering applications.
4. The univariate analysis and optimized tool of ANN programme for WEDM process parameters were provided guidelines for effective process parameters of WEDM process. This parameters selection helped the manufacturing engineers to maximize Al/SiC_{10%} MMC utilization for industrial applications for higher machining performances.
12. H Nakada, T Choh and N Kanetake, 'Fabrication and Mechanical properties of in situ Formed Carbide Particulate Reinforced Aluminium Composites. ' Journal of Metal Sciences, vol 30,
13. A. Manna and B. Bhattacharyya, (2003), "Taguchi method based parametric study of CNC-wire cut-EDM during machiing of Al/SiC-MMC, IE(I) Journal ,1 , 62-66.
14. R Ramakrishnan, L Karunamoorthy, Modelling and multi-response optimization of Inconel 718 on machineing of CNC WEDM process. Journal of material processig technology 207 (2008) 343-349.
15. Hilbert Schenck, Jr., Theories of engineering experimentation. pp.85-113,1998
16. S. K. Undirwade, M.P. Singh, C.N. sakhale,V. N. Bhaiswar,V.m. Sonde," Experimental & Dimensional Analysis Approach For Design Of Human Powered Bamboo Sliver Cutting" International Journal Of Engineering Science & Advanced Technology Volume-2, Issue-5, 1522 – 1527

REFERENCES

1. W Zhou and A M Xu. Casting of SiC Reinforced MMC's Journal of Material Process Technology, Vol 63, 1997. p 358.
2. L.A. Looney, J.M. Monaghan, P. O'Reilly and D.M.R. Taplin, The turning of an Al/SiC metal-matrix composite, Journal of Materials Processing Technology, 33 (1992) 453-468
3. O. Quigley, J. Monaghan, P. O'Reilly , Factors affecting the machinability of an Al/SiC metal-matrix composite, J. Mater. Process. Technol. 43 (1994) 21-36
4. A. Manna, B. Bhattacharayya , A study on machinability of Al/SiC-MMC, Journal of Materials Processing Technology 140 (2003) 711–716
5. S. Sarkar, S. Mitra, B. Bhattacharyya, (2005), "Parametric analysis and optimization of wire electrical discharge machining of γ -titanium aluminide alloy", Journal of Materials Processing Technology, 159, 286–294.
6. B. H.Yan, Tsai, H. C.Huang, F. Y., Long, L. Chorng. (2005), "Examination of wire electrical discharge machining of Al₂O₃p/6061Al composites", International Journal of Machine Tools & Manufacture, 45, 251–259.
7. M.Rozenek, and J. Kozak, (2001), "Electrical discharge machining characteristics of metal matrix composites", Journal of Materials Processing Technology, 109, 367-370.
8. Biing Hwa Yan, Hsien Chung Tsai, Fuang Yuan Huang, Long Chorng Lee; Examination of wire electrical discharge machining of Al₂O₃% /6061Al composites ; International Journal of Machine Tools & Manufacture 45 (2005) 251–259
9. Scot D, Boyina S., rajurkar K. P. , Analysis and optimization of parameter combinations in wire electrical discharge machining , Int. J. Prod. Res. 29 (11)(1991) 2189-2207
10. Y. S.Tang, S. C. Ma, L. K.chung, Determination of optimal cutting parameters in wire electrical discharge machining ,Int. J. Mech. Tool manuf. 35 (12) (1995) 1693-1701
11. D.B. Miracle, Metal matrix composites – From science to technological significance. Composite science and technology 65(2005) 2526-2540.